Neuron, Vol. 34, 463–477, April 25, 2002, Copyright ©2002 by Cell Press

The Acid-Activated Ion Channel ASIC Contributes to Synaptic Plasticity, Learning, and Memory

John A. Wemmie,[1,6] Jianguo Chen,[2,7] Candice C. Askwith,[3,5] Alesia M. Hruska-Hageman,[3,5] Margaret P. Price,[3] Brian C. Nolan,[4] Patrick G. Yoder,[3] Ejvis Lamani,[1] Toshinori Hoshi,[2,8] John H. Freeman, Jr.,[4] and Michael J. Welsh[2,3,5,9]

[1]Department of Psychiatry
[2]Department of Physiology and Biophysics
[3]Department of Internal Medicine
[4]Department of Psychology
[5]Howard Hughes Medical Institute
University of Iowa
Iowa City, Iowa 52242
[6]Department of Veterans Affairs Medical Center
Iowa City, Iowa 52242
[7]Department of Pharmacology
Tongji Medical College, Huazhong
University of Science and Technology
Wuhan
China
[8]Department of Physiology
University of Pennsylvania
Philadelphia, Pennsylvania 19104

Summary

Many central neurons possess large acid-activated currents, yet their molecular identity is unknown. We found that eliminating the acid sensing ion channel (ASIC) abolished H^+-gated currents in hippocampal neurons. Neuronal H^+-gated currents and transient acidification are proposed to play a role in synaptic transmission. Investigating this possibility, we found ASIC in hippocampus, in synaptosomes, and in dendrites localized at synapses. Moreover, loss of ASIC impaired hippocampal long-term potentiation. ASIC null mice had reduced excitatory postsynaptic potentials and NMDA receptor activation during high-frequency stimulation. Consistent with these findings, null mice displayed defective spatial learning and eyeblink conditioning. These results identify ASIC as a key component of acid-activated currents and implicate these currents in processes underlying synaptic plasticity, learning, and memory.

Introduction

Acid-activated cation currents have been detected in central and peripheral neurons for more than 20 years (Gruol et al., 1980; Krishtal and Pidoplichko, 1981). Despite the wide spread distribution of H^+-gated currents in the brain (Escoubas et al., 2000; Vyklicky et al., 1990), neither their molecular identity nor their physiologic functions are known.

The ability of acid to activate three members of the DEG/ENaC cation channel family suggest they might be responsible for H^+-gated currents in the central nervous system. Subunits of the DEG/ENaC protein family associate as homomultimers and heteromultimers to form voltage-insensitive channels. Individual subunits share a common structure with two transmembrane domains, intracellular carboxyl and amino termini, and a large, cysteine-rich extracellular domain thought to serve as a receptor for extracellular stimuli. Most DEG/ENaC channels are inhibited by the diuretic amiloride. The three mammalian acid-activated DEG/ENaC channels are brain Na^+ channel 1 (BNC1, also called MDEG, BNaC1, ASIC2), acid sensing ion channel (ASIC, also called BNaC2, ASIC1), and dorsal root acid sensing ion channel (DRASIC, also called ASIC3) (Price et al., 1996; Waldmann et al., 1996, 1997a, 1997b; García-Añoveros et al., 1997; Waldmann and Lazdunski, 1998). BNC1 and ASIC each have alternatively spliced isoforms (BNC1a and 1b, and ASICα and ASICβ) (Chen et al., 1998; Lingueglia et al., 1997; Price et al., 2000). Heterologous expression of most of these subunits generates Na^+ currents that activate at low extracellular pH and then desensitize in the continued presence of acid (Benson et al., 2002; Waldmann and Lazdunski, 1998). Expression of individual subunits and coexpression of more than one subunit generates currents that show distinct kinetics and pH sensitivity.

Based on the transient nature of H^+-evoked currents in primary cultures of cortical neurons and their inhibition by amiloride, Varming (Varming, 1999) suggested that DEG/ENaC channels and ASIC in particular might be responsible for the endogenous H^+-gated currents. The pattern of expression was consistent with this idea; ASICα, BNC1a, and BNC1b have transcripts in the central nervous system (García-Añoveros et al., 1997; Price et al., 1996; Waldmann et al., 1997b), whereas DRASIC and ASICβ are expressed primarily in the peripheral nervous system (Chen et al., 1998; Waldmann et al., 1997a). ASIC transcripts were most abundant in the cerebral cortex, hippocampus, cerebellum, and olfactory bulb (García-Añoveros et al., 1997; Waldmann et al., 1997b). A recent study reported that a peptide toxin from South American tarantula *Psalmopoeus cambridgei* inhibited ASIC and acid-evoked currents in cultured cerebellar granule cells (Escoubas et al., 2000), further suggesting that ASIC could be a component of pH-gated currents.

There has been speculation about the physiologic and pathophysiologic function of acid-gated currents in central neurons. It has been hypothesized that interstitial acidosis associated with seizures and ischemia could trigger their activity, thereby exacerbating the pathological consequences of these conditions (Varming, 1999; Waldmann et al., 1997b). Although macroscopic changes in extracellular pH in the brain are tightly controlled by homeostatic mechanisms (Chesler and Kaila, 1992), it is possible that pH fluctuations in specific micro-domains such as the synapse may be significant (Waldmann et al., 1997b). For example, the acid pH of synaptic vesicles has been suggested to transiently influence local extracellular pH upon vesicle release (Krishtal et al., 1987; Waldmann et al., 1997b). Consistent with this idea, tran-

[9]Correspondence: mjwelsh@blue.weeg.uiowa.edu

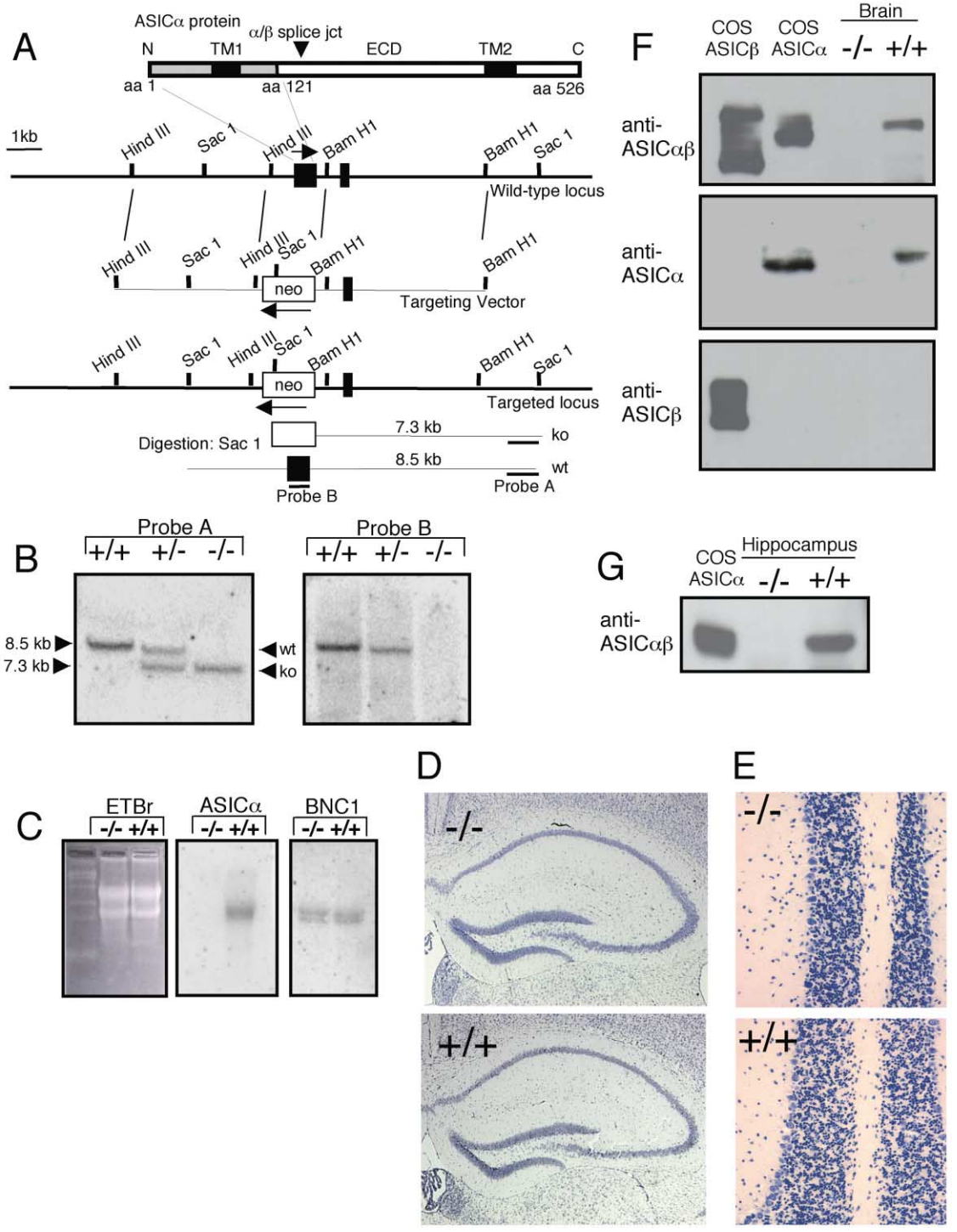

Figure 1. Generation of ASIC Knockout Mice

(A) The top bar illustrates the anticipated topology of the ASIC protein (N, amino terminus; C, carboxyl terminus; TM, transmembrane domain; ECD, extracellular domain; stippled region is coded by targeted exon; arrowhead, splice junction). Also shown are wild-type genomic locus, targeting vector, and targeted locus. (B) Southern blot analysis demonstrates disruption of the *ASIC* gene. Genomic DNA was SacI digested and hybridized to a probe outside of the targeting vector (probe A) or to a probe corresponding to the deleted exon (probe B). (C) Total brain RNA was subjected to Northern blot analysis and hybridized to a probe for *ASIC*α or *BNC1*. Equivalent loading of RNA was verified by ethidium bromide (ETBr) staining of ribosomal RNA. (D and E) Nissl staining was performed on 5 μm coronal sections through the hippocampus and cerebellar cortex, respectively. (F) Immunoprecipitation was performed on whole brain extracts with anti-ASICαβ anti-sera; this was then Western blotted with the antibodies indicated on the left. Equivalent amounts of total protein from −/− and +/+ mice were used as starting material. As a positive control for ASICα and ASICβ, protein extracts were used from COS cells transfected with the respective cDNAs. Nontransfected COS cells yielded no signal when probed with anti-ASIC antibodies (not shown). (G) Immunoprecipitation and Western blotting were performed on extracts from dissected hippocampus using anti-ASICαβ sera.

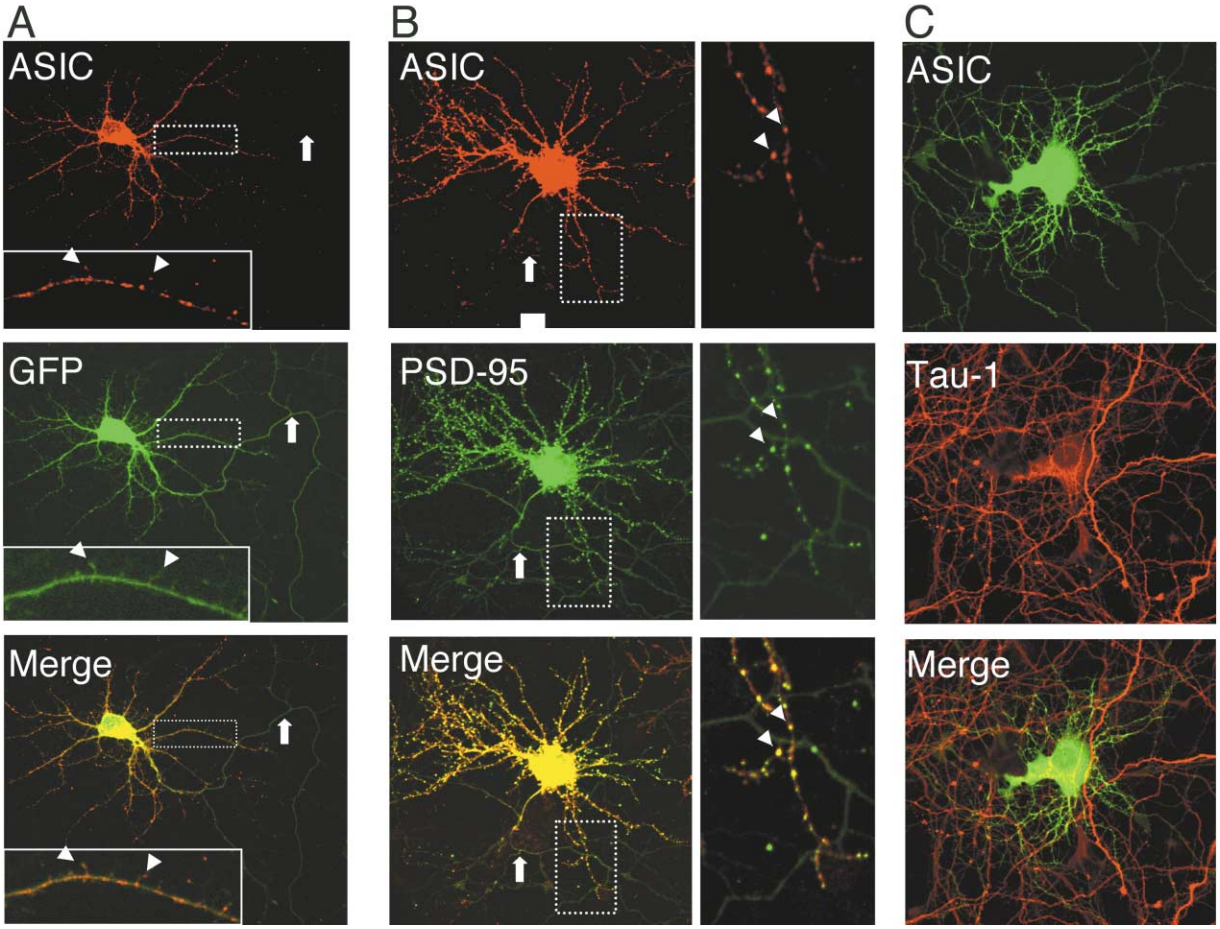

Figure 2. Distribution of ASIC in Transfected Rat Hippocampal Neurons

(A) ASIC is distributed in a punctate pattern (ASIC-FLAG immunofluorescence, red; GFP fluorescence, green). The arrow indicates a process that lacks ASIC immunofluorescence but is positive for GFP. Inset is enlargement of area marked by dashed rectangle. Arrowheads point to ASIC signal at tips of dendritic spines. (B) ASIC and PSD-95 are colocalized (ASIC-FLAG immunofluorescence, red; PSD-95-GFP fluorescence, green). Arrow indicates a process with little ASIC immunofluorescence but some PSD-95 staining which is less punctate than in other processes. Images to right show areas enclosed by dashed rectangles. Arrowheads indicate examples of puncta where ASIC and PSD-95 are colocalized. (C) ASIC-GFP fluorescence (green) and axonal dephospho-tau-1 immunostaining (red) do not overlap.

sient acidification of extracellular pH has been recorded with synaptic transmission in cultured hippocampal neurons (Miesenbock et al., 1998) and in hippocampal slices (Krishtal et al., 1987). Thus it has been proposed that H^+-gated currents may provide a target for protons released during synaptic transmission and thus play a role in the physiology of synaptic transmission (Krishtal et al., 1987; Waldmann et al., 1997b).

Therefore, to understand the role of H^+-gated currents in central neurons in general, and the role of ASIC in particular, we generated mice with a targeted disruption of the *ASIC* gene. We then tested the hypothesis that ASIC contributes to neuronal acid-gated currents and to synaptic function and behavior.

Results

Targeted Disruption of the Mouse *ASIC* Gene

ASIC knockout mice were generated by deleting a region of genomic DNA encoding the first 121 amino acids of ASICα. This region includes the intracellular N terminus, the first transmembrane domain, and a portion of the extracellular domain of the ASICα protein. The wild-type locus, targeting vector, and targeted locus are shown schematically in Figure 1A. Southern hybridization of Sac1 digested genomic DNA with the flanking probe demonstrated targeted integration (Figure 1B, probe A). Southern and Northern hybridization confirmed targeted integration, and disruption of ASIC but not BNC1 mRNA (Figures 1B and 1C). ASIC knockout mice showed normal viability, size, appearance, fertility, life span, and motor and behavioral activity. Brain morphology and neuron appearance and distribution in the hippocampus were also normal in $-/-$ mice (Figures 1D and 1E).

We tested for ASIC protein in brain using an antibody against the intracellular carboxyl terminus (anti-ASIC$\alpha\beta$); this antibody recognizes both ASICα and ASICβ (Figure 1F). Immunoprecipitation and Western blotting detected ASIC in protein extracts of whole brain and hippocampus of $+/+$ but not $-/-$ animals (Figures 1F and 1G). We also detected protein when anti-ASIC$\alpha\beta$ immuno-

precipitates were probed with an antibody specific for ASICα (anti-ASICα), but not with an antibody specific for ASICβ (anti-ASICβ). These data suggest that the ASICα isoform is much more abundant in mouse brain than ASICβ, consistent with the previous finding that ASICβ transcripts are not detected in rat brain (Chen et al., 1998). These data also show the loss of ASIC protein in −/− animals.

ASIC Colocalizes with PSD-95 in Hippocampal Neurons and Synaptosome-Enriched Subcellular Fractions

To investigate the location of ASIC, we transfected cultured hippocampal neurons with an epitope-tagged ASICα and examined its distribution. ASIC-specific immunostaining was detected in the cell body and in a punctate pattern in processes both proximally and distally (Figures 2A, 2B, and 2C). ASIC-containing puncta were present on both dendritic shafts and the termini of dendritic spines (Figure 2A). The localization of ASIC coincided in large part with that of cotransfected PSD-95 linked to GFP (Figure 2B); this fusion protein exhibits a synaptic pattern of distribution (Craven et al., 1999). To test whether ASIC distribution was dependent on exogenous PSD-95 expression, we examined ASIC localization in cells cotransfected with GFP alone (Figure 2A); ASIC remained punctate while GFP distributed diffusely throughout the neuron. Likewise, ASIC transfected alone showed the same punctate distribution (not shown). ASIC staining was much less pronounced in processes with features of axons (Figures 2A and 2B, arrows); i.e., those processes tended to be longer, less numerous, and with right angle branching (Stowell and Craig, 1999). Likewise, PSD-95 which is normally distributed to dendrites was more diffuse and less punctate when detected in these processes (Figure 2B). Moreover, we did not observe colocalization of ASIC and the axonal marker dephospho tau-1 (Figure 2C) (Mandell and Banker, 1996). These results suggest that in hippocampal neurons, ASIC is located at dendritic synapses, and thus is likely present in the postsynaptic membrane.

To explore whether endogenously expressed ASIC protein is distributed similarly to PSD-95, we prepared synaptosome-enriched subcellular fractions of brain. As described by others (Cho et al., 1992), these fractions are enriched in both pre- and postsynaptic proteins. Both PSD-95 and GluR2/3 were increased in synaptosome-enriched fractions (Figure 3A) (Cho et al., 1992). Likewise, ASIC showed substantial enrichment in the synaptosome-containing fractions (Figure 3A). ASIC and PSD-95 segregated similarly in each of the subcellular fractions analyzed (Figure 3B). These data support the results obtained by immunostaining (Figure 2) and suggest that similar to PSD-95, ASIC is present at synapses.

ASIC Contributes to Acid-Evoked Currents in Hippocampal Neurons

We tested the hypothesis that ASIC contributes to the acid-evoked currents previously reported in hippocampal neurons (Varming, 1999; Vyklicky et al., 1990). Acid application generated a transient current in 93% (n = 76) of neurons from +/+ mice (Figure 4A), but in striking contrast, pH 5 failed to activate analogous currents in

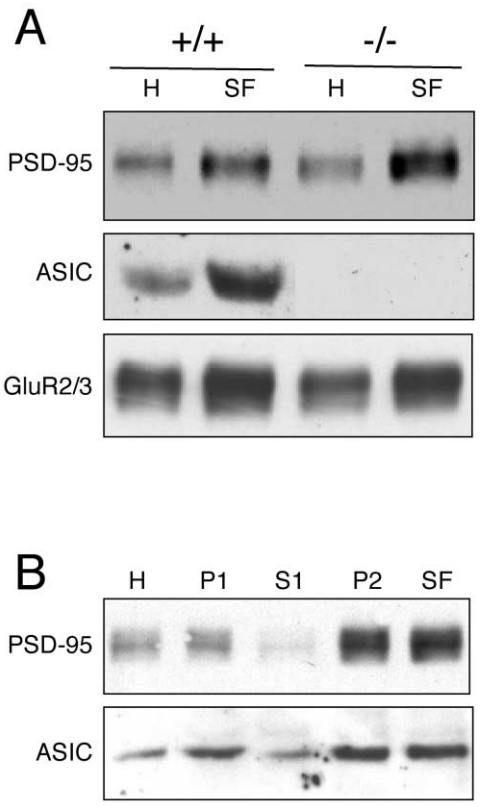

Figure 3. ASIC Is Enriched in Synaptosome-Containing Brain Fractions

(A) Western blotting was performed on protein fractions from brain of wild-type and ASIC knockout mice using antibodies to ASIC, PSD-95, and GluR2/3 (indicated on left). (B) Shown is Western blotting for PSD-95 and ASIC in the additional subcellular fractions from brain of wild-type mice (Homogenate, H; 1000 × g pellet, P1 and supernatant, S1; 12,000 × g pellet, P2; synaptosomal fraction, SF). Equivalent amounts of protein were loaded in each lane.

neurons from −/− mice (n = 99). Currents activated by GABA, AMPA, and NMDA and the voltage and Mg^{2+} dependence of NMDA receptor currents appeared normal in −/− neurons (Figures 4A, 4B, and 4C). These data indicate that ASIC is a required component of the channels that respond to acid in hippocampal neurons.

Baseline Synaptic Transmission in the Hippocampus Is Normal in ASIC Knockout Mice

The absence of H^+-gated currents in hippocampal neurons of −/− animals provided the opportunity to assess their physiologic significance in the hippocampus. To explore their potential function at hippocampal synapses, we tested synaptic transmission at Schaffer collateral-CA1 synapses in hippocampal slices. In the presence of 1.3 mM Mg^{2+}, field excitatory postsynaptic potentials (fEPSPs) for the two genotypes were similar in slope, amplitude, and response to increasing stimulus intensity (Figures 5A, 5B, and 5D); under these conditions, fEPSPs reflect primarily AMPA-mediated currents. In the presence of a low Mg^{2+} concentration, the slope and amplitude of fEPSPs and the ratios of total fEPSP

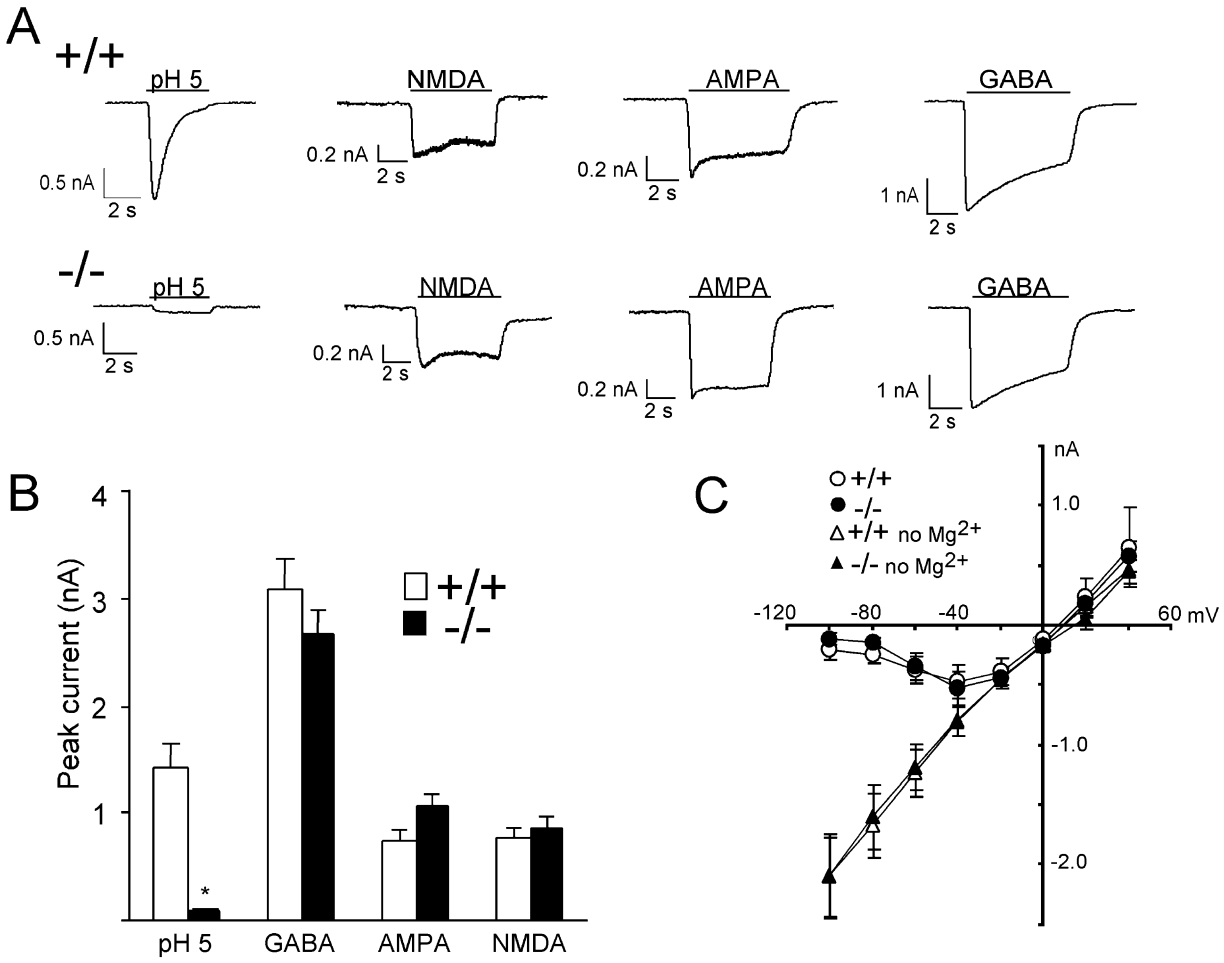

Figure 4. Transient Acid-Evoked Cation Currents Are Absent in Hippocampal Neurons from ASIC Knockout Mice

(A) Tracings are representative whole cell recordings of pyramidal neurons from +/+ and −/− mice in response to application of 200 μM of indicated agonist. (B) Bar graph illustrates average peak currents elicited by indicated agonist. Asterisk indicates $p < 0.00001$. Differences in response of +/+ and −/− neurons to GABA, AMPA, and NMDA were not statistically significant (+/+, n = 32; −/−, n = 41). (C) NMDA-mediated currents were analyzed for voltage dependence in the presence and absence of Mg^{2+} from +/+ (n = 5) and −/− (n = 9) neurons. Error bars represent SEM.

to the NMDA component were similar in +/+ and −/− animals (Figures 5A and 5C). These results suggested that synaptic transmission at baseline was not affected by the loss of ASIC.

Impairment of Long-Term Potentiation in ASIC Knockout Mice

LTP at Schaffer collateral-CA1 synapses represents one form of synaptic plasticity and serves as a molecular model for specific types of learning and memory (Bliss and Collingridge, 1993; Malinow et al., 2000). Immediately following LTP induction with high-frequency stimulation (HFS), slices from both genotypes showed an increase in fEPSP slope and amplitude. This result suggests that short-term potentiation (STP) occurs in both groups (Figure 5D), although the degree of STP was slightly less in the −/− group. In contrast, long-term potentiation was strikingly impaired in the −/− mice. By 40 min after HFS, the fEPSPs from −/− mice had decayed to baseline whereas fEPSPs from +/+ mice remained potentiated. By 55 min., the fEPSPs in the ASIC null slices remained at pre-HFS baseline values (not shown). This result indicates that ASIC and H^+-gated currents may play a specific role in the development or maintenance of LTP.

A central feature of CA1 LTP is activation of the NMDA receptor due to binding of the neurotransmitter glutamate and to depolarization of the postsynaptic membrane through the release of voltage-dependent Mg^{2+} block (Bliss and Collingridge, 1993; Malinow et al., 2000). To determine whether the loss of ASIC might impact this process, we repeated the LTP experiments with a low Mg^{2+} concentration (0.1 mM) in the bathing solution. Previous work has shown that low Mg^{2+} concentrations facilitate LTP by promoting activation of the NMDA receptor (Huang et al., 1987). Following HFS in the presence of low Mg^{2+}, both genotypes exhibited comparable LTP (Figure 5E). Thus the reduced Mg^{2+} concentration restored LTP in the −/− slices. This result suggests that facilitating NMDA receptor function may be sufficient to overcome the ASIC-dependent deficit in LTP.

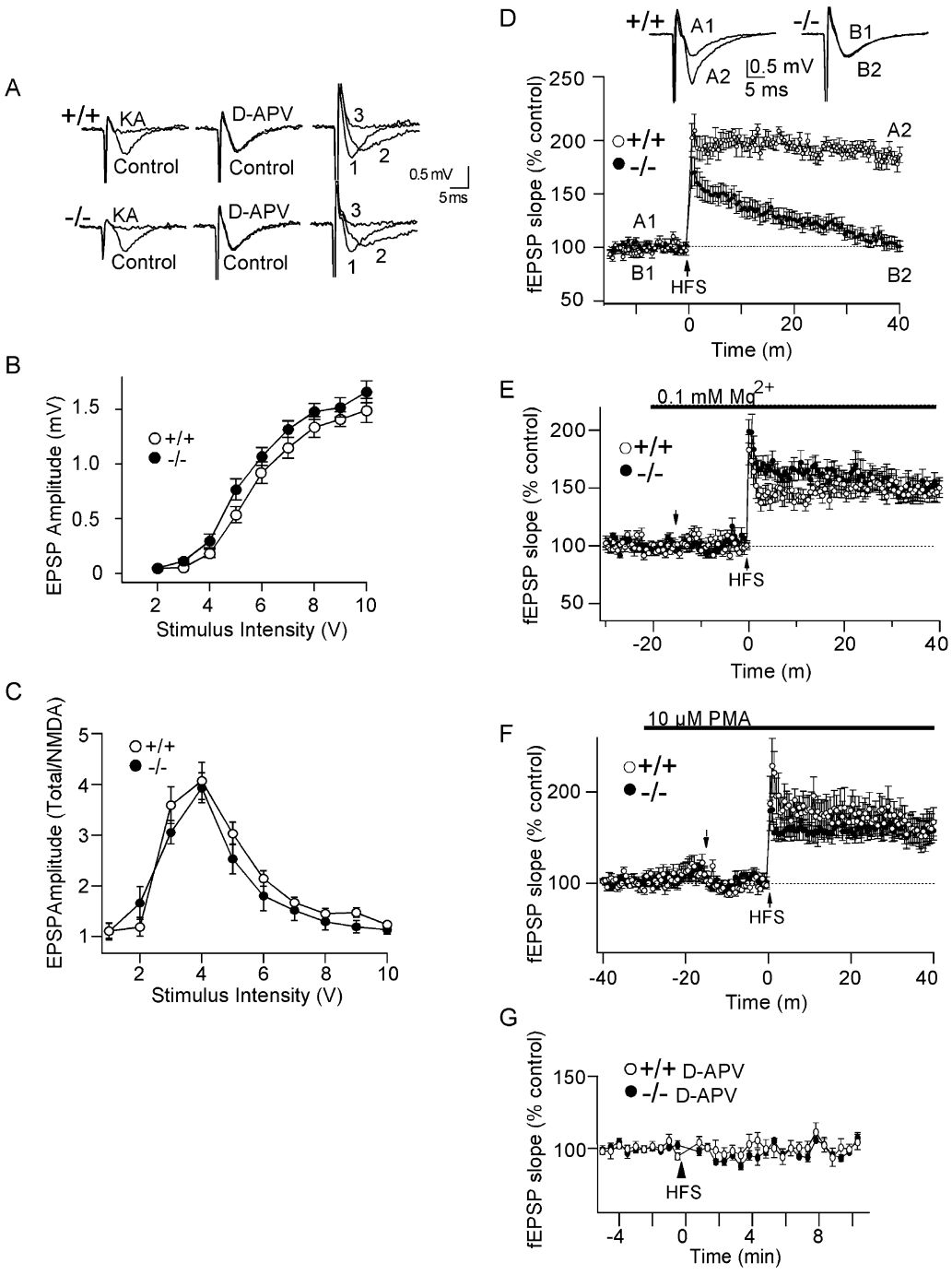

Figure 5. Baseline Synaptic Transmission Is Normal and LTP Is Impaired in Hippocampal Slices from ASIC Knockout Mice

(A) Tracings represent the baseline components of the EPSP. Left column, the nonspecific ionotropic glutamate receptor antagonist kynurenic acid (KA) (5 mM) abolished EPSPs in slices from +/+ and −/− mice. Middle column, the NMDA receptor antagonist D-2-amino-5-phosphopentanoic acid (D-APV) (50–100 μM) did not significantly change the EPSPs from either +/+ or −/−mice under the conditions used for the LTP experiments (1.3 mM Mg^{2+}). Right column, the AMPA receptor antagonist 6-cyano-7-nitroquinoxaline-2,3-dione (CNQX) and D-APV abrogate the baseline EPSP. EPSPs from +/+ and −/− mice were recorded in the presence of (1) 1.3 mM Mg^{2+}, (2) 0.1 mM Mg^{2+}, and 10 μM CNQX, or (3) 0.1 mM Mg^{2+}, 10 μM CNQX, and 50 μM D-APV. The non-CNQX-sensitive component of the EPSP was not different between groups and in both groups the EPSP was blocked by CNQX plus D-APV. These experiments were repeated on three separate preparations, and quantitative results for the various components are shown in panels (B) and (C). (B) EPSP amplitude plotted as a function of stimulus intensity shows no significant difference between slices from +/+ and −/− mice. Bathing medium contained 1.5 mM Mg^{2+} (+/+, n = 15; −/−, n = 15). (C) Shown is the ratio of total fEPSP amplitude to fEPSP in the presence of CNQX (10 μM), both in 0.1 mM Mg^{2+} (n = 6 +/+ and 5 −/− mice). Values were not significantly different. (D) LTP is impaired in −/− slices. Average normalized EPSP slope is plotted versus time. A1, A2, B1, B2 are representative tracings at indicated times. HFS represents the application of 100 Hz. for 1 s (+/+, n = 8; −/−, n = 13). Forty minutes after HFS, the average fEFSP slope was 99 ± 5 % of pre-HFS values in −/− mice and 184 ± 7 % of pre-HFS values in +/+ mice,

Another component of LTP generation is activation of PKC (Ben-Ari et al., 1992). One effect of PKC activation in the CA1 area of the hippocampus is on the Ca^{2+}-dependent regulation of the NMDA receptor (Chen and Huang, 1992). Previous studies demonstrated that phorbol esters enhanced field EPSPs, but at higher doses blocked additional potentiation induced by HFS (Kleschevnikov and Routtenberg, 2001; Malenka et al., 1986); this probably represents a form of occlusion. To find a dose of phorbol ester that did not occlude LTP, we examined a dose-response relationship between phorbol 12-myristate 13-acetate (PMA) concentration and baseline transmission (not shown). At higher doses, PMA potentiated baseline EPSP slope and amplitude. However, 10 μM PMA did not affect baseline transmission in most slices; in a few cases where potentiation did occur with 10 μM PMA, reducing the stimulus intensity permitted a stable baseline transmission (Figure 5F). Following HFS in the presence of 10 μM PMA, LTP was restored in the −/− slices (Figure 5F). Like the experiments using a low Mg^{2+} concentration, this result suggests that in the absence of ASIC, LTP induction may require the enhancement of another component of the system.

Activation of the NMDA receptor during HFS is critical for LTP induction. For example, 50 μM D-APV blocked induction of both LTP and STP in +/+ and −/− mice (Figure 5G). Interestingly, others have shown that a partial blockade of the NMDA receptor with D-APV prevents LTP but spares short-term potentiation (Malenka, 1991). This situation resembles our results in which the loss of ASIC prevented LTP, but not short-term potentiation (Figure 5D). Finding that LTP was rescued in ASIC −/− mice by augmenting NMDA receptor function (Figure 5E) suggested the hypothesis that ASIC may contribute to NMDA receptor activation during LTP induction. Therefore, we examined fEPSPs during high-frequency stimulation. In wild-type slices, fEPSP amplitude was facilitated during the initial period of HFS; relative to the first EPSP, the amplitudes of the next seven EPSPs were increased (Figures 6A–6C). In ASIC null mice, the facilitation during HFS was markedly attenuated (Figures 6A–6C). To investigate whether inadequate NMDA receptor activation could account for the impaired facilitation, we applied D-APV to wild-type slices prior to HFS. The pattern of EPSP facilitation elicited by blocking the NMDA receptor showed a remarkable resemblance to that obtained in ASIC null slices (Figures 6A, 6B, and 6D). Moreover, D-APV had no detectable effect on EPSP facilitation in the ASIC null slices (Figures 6A and 6D.) Thus ASIC-dependent facilitation of NMDA receptor function could account for the impact of ASIC disruption on LTP.

Paired Pulse Facilitation Is Normal in ASIC Null Mice

Paired pulse facilitation serves as a commonly used index of presynaptic activity and neurotransmitter release probability (Schulz et al., 1994). We found comparable paired pulse facilitation in animals of both genotypes (Figures 6E and 6F). Moreover, as expected, D-APV had no effect on paired pulse facilitation (not shown). These experiments suggest that presynaptic neurotransmitter release is normal in the ASIC knockout mice.

ASIC Null Mice Exhibit a Mild and Reversible Deficit in Spatial Learning and Memory

NMDA receptor-dependent synaptic plasticity in the CA1 region of the hippocampus has a key role in the acquisition and consolidation of spatial memory (Tsien et al., 1996). Impaired synaptic plasticity in ASIC knockout mice suggested they might show a defect in hippocampus-dependent spatial learning. To test this, we used the hidden platform version of the Morris water maze (Morris, 1981). In this test, mice must learn the position of a submerged hidden platform relative to visual cues outside the pool. Naive mice received a single trial per day for 11 consecutive days. Escape latencies of both +/+ and −/− mice improved significantly during the course of training (Figure 7A). However, beyond day 3, the +/+ group was significantly faster at locating the platform than the −/− group. These results indicate that although the −/− mice could learn to find the location of the platform, their memory was less stable, resulting in poorer retention from one training day to the next.

At the end of the training protocol, a probe trial was performed to examine whether mice had used spatial learning strategies to find the platform rather than other nonspatial strategies. We found subtle differences in the performance of null mice during the probe trial (Figures 7B and 7C). Although there was not a statistically significant difference between the performance of +/+ and −/− mice in probe trial performance, the +/+ mice spent a significantly greater amount of time in the training quadrant than in any of the other quadrants (Figure 7B). In contrast, the amount of time ASIC −/− animals spent in the training quadrant was not significantly different from that spent in the other quadrants (Figure 7B). An analysis of the number of platform crossings yielded similar results (Figure 7C). Following the probe trial, a two trial platform reversal test was performed. In the first trial, the platform was returned to the original training quadrant. In the second trial, the platform was switched to the opposite quadrant. Wild-type mice located the platform when it was in the training quadrant

$p = 0.000005$. Fifty-five minutes after HFS, the EPSPs in the knockout slices remained 102 ± 3% ($n = 3$) of pre-HFS values (not shown). (E) LTP is rescued in −/− slices in the presence of low Mg^{2+} (0.1 mM, bar) (+/+, $n = 6$; −/−, $n = 6$). Mean EPSP values 40 min after HFS in +/+ and −/− mice were 152 ± 5% and 156 ± 8% baseline, respectively ($p = 0.99$). As expected, a reduction in Mg^{2+} concentration caused a slight increase in baseline EPSP slope in both groups of mice. To maintain comparable baseline transmission, the stimulus intensity was reduced slightly in both groups 15 min prior to HFS (downward arrow). (F) Application of phorbol 12-myristate 13-acetate (10 μM PMA, bar) restores LTP in −/− slices (+/+, $n = 6$; −/−, $n = 5$). Mean EPSP amplitudes at 40 min following HFS were not different (−/−, 158 ± 11%; +/+, 167 ± 15%; $p = 0.41$). When we activated PKC in the brain slice by the addition of PMA, baseline EPSP amplitude increased slightly in 2 of 6 slices from the −/− group and 1 of 5 slices from the +/+ group. Increases in baseline EPSP were corrected by decreasing stimulus intensity (downward arrow). A stable EPSP baseline was observed for 15 min before HFS. (G) D-APV blocked STP and LTP induction both in +/+ mice and −/− mice. Slices were incubated in the presence of 50 μM D-APV for at least 20 min prior to HFS (+/+, $n = 5$; −/−, $n = 5$).

significantly faster than when it was in the opposite quadrant (Figure 7D). In contrast, the times required for the knockout mice to locate the platform in the training and in the opposite quadrant were not statistically different (Figure 7D). Taken together, these results suggest that the ASIC −/− mice have a subtle deficit in spatial memory.

Others have demonstrated that intensive training can normalize subtle learning deficits (Abeliovich et al., 1993). Therefore we asked whether an intensified training protocol could reverse the spatial learning deficit in the null mice. When the mice underwent three blocks of four trials per day for three consecutive days, we found that the performance of the +/+ and −/− groups were indistinguishable both in terms of escape latency (Figure 7E) and probe trials (not shown). Thus, more intensive training reversed the ASIC-dependent spatial learning deficit in the null mice.

Loss of ASIC Impairs Eyeblink Conditioning

In addition to the hippocampus, ASIC transcripts are also expressed in granule and Purkinje cells in the cortex of the cerebellum (García-Añoveros et al., 1997; Waldmann et al., 1997b). Synapses between granule and Purkinje cells are likely sites for associative learning in classical eyeblink conditioning (Thompson and Kim, 1996). Thus we asked whether loss of ASIC affected eyeblink conditioning. The basic procedure for eyeblink conditioning involves the paired presentation of an innocuous conditioned stimulus (CS) such as a tone, followed by a noxious unconditioned stimulus (US) such as a periorbital shock. With training, an association is made between the CS and the US so that a conditioned response (CR) is acquired. The coordinated motor response of the CR includes eyelid closure and is precisely timed to occur just prior to the delivery of the shock. Animals given unpaired presentations of CS and US do not develop the eyeblink CR, and thus serve as a control for nonassociative sources of behavioral responses.

Although mice of both genotypes developed associative conditioning, the +/+ mice developed significantly stronger eyeblink conditioning than did the −/− mice (Figure 8A). After five training sessions, the tone generated a conditioned response approximately 80% of the time in wild-type mice, whereas ASIC null mice showed a conditioned response only about 50% of the time. The response percentage in the unpaired condition was not different between genotypes (Figure 8A). Likewise, there was no significant difference in the amplitude of the unconditioned eyeblink response during the pre-training session. These results indicate that the impaired conditioning in the ASIC −/− mice was not due to a performance deficit. Thus, as with spatial memory, the strength of eyeblink conditioning was impaired in the ASIC null mice.

To determine whether other cerebellum-dependent tasks were affected, we compared ASIC −/− and +/+ mice on the accelerating rotarod (Figure 8B). The performance of the two groups was indistinguishable. Previously it has been shown that manipulations such as disrupting the glial fibrillary acidic protein (GFAP) or inhibition of PKC can affect cerebellar plasticity and eyeblink conditioning or the vestibulo-ocular reflex but do not lead to impaired performance on the rotating rod (De Zeeuw et al., 1998; Shibuki et al., 1996). Similar to these manipulations, the ASIC null mutation may affect specific forms of learning and plasticity.

Because ASIC is also expressed in sensory neurons (Chen et al., 1998; Waldmann et al., 1997a), a potential confounding factor in our behavioral studies could be a loss of peripheral sensory function (Price et al., 2000). However, we tested mechanical and thermal sensation at the behavioral level and found no difference compared to littermate controls (not shown). This result agrees with the normal unconditioned eyeblink response (UR). In addition, the rotating rod provides a general test of coordination, strength, stamina, motivation, activity, and sensory function. The normal performance of the mutant mice in this task suggests that these characteristics are not grossly impaired. Together these observations suggest that the observed differences in learning in the −/− mice are not likely the result of sensory or performance deficit.

Discussion

These data provide, at least in part, a molecular identity to the H^+-gated currents that for many years have been observed in central neurons (Escoubas et al., 2000; Varming, 1999; Vyklicky et al., 1990). Additionally, these studies provide insight into the physiologic importance of these poorly understood channels.

The absence of H^+-gated currents in ASIC null neurons was surprising because BNC1 expression was normal (Figure 1C) and because previous studies in heterologous cells showed that ASIC and BNC1 subunits can associate as either homo- or hetero-multimers to produce acid-evoked currents (Bassilana et al., 1997; Benson et al., 2002). Our data suggest either that ASIC is the only DEG/ENaC channel responsible for H^+-activated currents in hippocampal neurons or that BNC1 is dependent on ASIC for some step in biosynthesis or function.

Contribution of ASIC to Synaptic Plasticity

We found ASIC enriched in synaptosomes, immunostaining detected ASIC at synapses in a pattern suggesting primarily a dendritic localization, and paired pulse facilitation was normal in ASIC −/− hippocampal slices. These results implicated a postsynaptic localization for ASIC and suggested ASIC might play an important role in synaptic function. Although disruption of the *ASIC* gene did not affect basal synaptic transmission, it impaired hippocampal LTP and facilitation during HFS. Thus, ASIC was required for normal synaptic plasticity.

Several observations suggest that ASIC may contribute to LTP induction by facilitating activation of the NMDA receptor, particularly during high-frequency stimulation. For example, the absence of ASIC and blockade of NMDA receptors generated similar effects on EPSP facilitation during HFS. The reduced effect of D-APV on HFS in the knockout mice is also consistent with hypoactive NMDA receptor function. Yet, clearly NMDA receptors were present and exhibited normal voltage dependence in cultured hippocampal neurons from ASIC −/− mice. NMDA receptor function was also revealed in ASIC null slices by the findings that D-APV

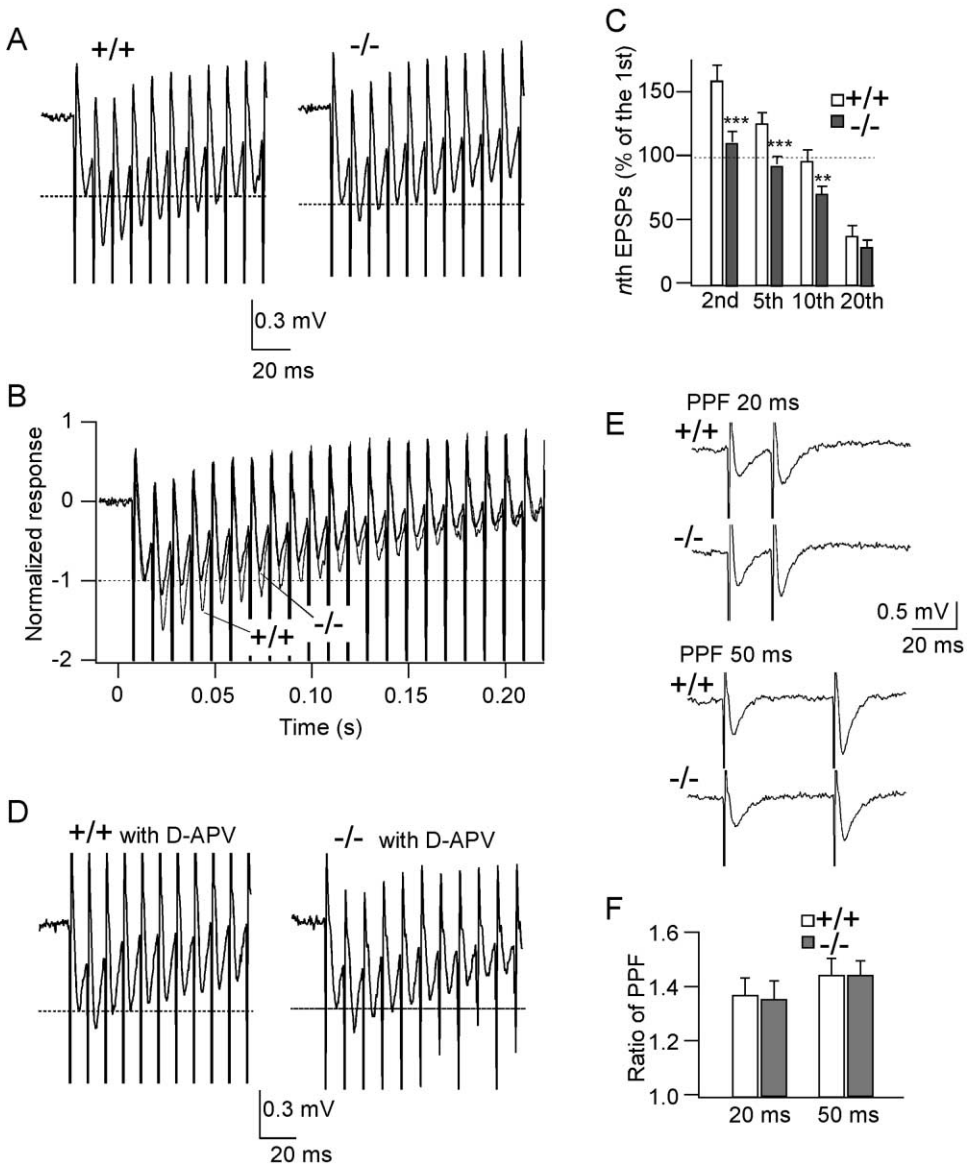

Figure 6. EPSP Facilitation during HFS Is Impaired but Paired Pulse Facilitation (PPF) Is Intact in ASIC −/− Mice

(A) Shown are the averaged responses of the first 10 EPSPs during HFS in +/+ mice (n = 8) and −/− mice (n = 8). (B) The normalized responses to HFS are superimposed; +/+ (thin tracing) and −/− mice (thick tracing). All the amplitudes of EPSP during HFS were normalized to the amplitude of the first EPSP in each slice. (C) Amplitude of 2nd, 5th, 10th, 20th EPSPs were normalized to the amplitude of the first EPSP. The 2nd, 5th, 10th EPSPs are significantly different between +/+ and −/− mice (***: $p < 0.001$, **: $p < 0.05$). (D) D-APV (50 μM) exhibits a greater effect on the high-frequency train in +/+ (n = 5) than −/− (n = 5) slices. Both tracings are similar to ASIC −/− slices without D-APV. (E) Paired pulse facilitation was similar in +/+ and −/− mice at both 20 and 50 ms intervals. (F) The averaged PPF ratio of +/+ (n = 21) and −/− mice (n = 22) was plotted for both the 20 and 50 ms intervals. There was no significant difference between +/+ and −/− mice; 20 ms ($p = 0.81$), 50 ms ($p = 0.93$).

blocked short-term potentiation and a low Mg^{2+} concentration or PKC activation rescued LTP. In addition, the NMDA receptor-mediated component of the EPSP at baseline was similar in +/+ and −/− slices in a low Mg^{2+} buffer.

By generating postsynaptic Na^+ channels, ASIC might promote membrane depolarization thereby facilitating release of the Mg^{2+} block of the NMDA receptor. It is also possible that an ASIC-mediated increase in intracellular Na^+ may increase NMDA receptor activity (Yu and Salter, 1998). Although less direct and perhaps less likely, it is possible that ASIC could influence one of the second messenger systems that affects NMDA receptor composition, activity, or trafficking. Further studies will be necessary to clarify the relationship between ASIC and NMDA receptor function and the impact on synaptic plasticity.

Accumulating evidence suggests a model in which release of vesicular protons modulates synaptic transmission (DeVries, 2001; Krishtal et al., 1987; Traynelis and Chesler, 2001; Varming, 1999; Waldmann et al., 1997b). Synaptic vesicles are acidic (pH ~5.7) (Miesen-

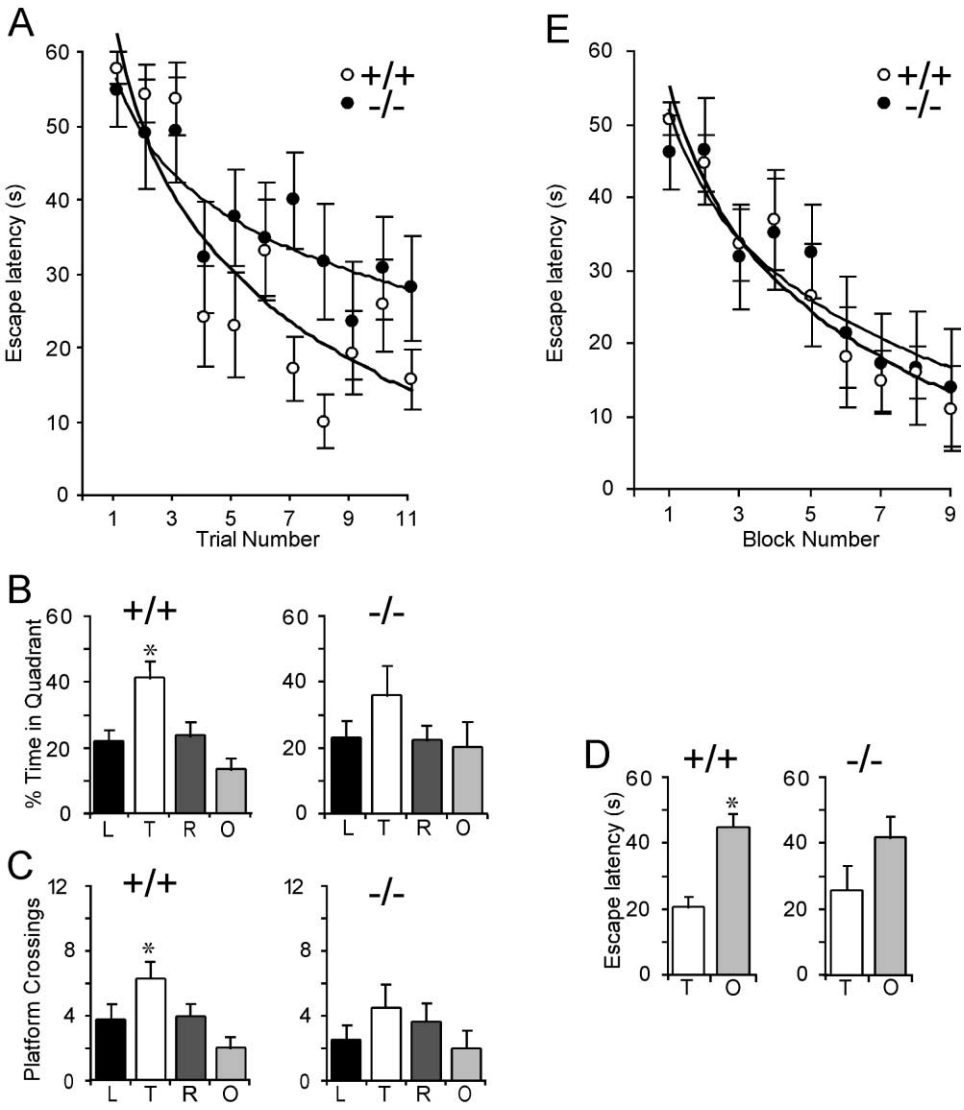

Figure 7. A Mild Deficit in Spatial Memory in ASIC Null Mice Can Be Overcome by Intensive Training

(A) Escape latency in the Morris water maze was plotted versus day of training. Mice underwent 1 trial per day for 11 days. Regression analysis of learning curves of two groups revealed a significant difference in slope ($t(131) = 2.93$; $p < 0.004$; +/+, n = 10; −/−, n = 9). Repeated measures analysis of variance with all 11 trials revealed a difference that was not within the standard confidence interval ($(F1,17) = 3.20$; $p < 0.095$), although analysis of variance of last five trials revealed a significant effect of group factor ($F(1,17) = 5.43$; $p < 0.035$). Due to the difference in learning curve slope, the difference in learning proficiency is more apparent with later trials. (B) The percentage of time spent in the indicated quadrant during the probe trial was analyzed; training, T; adjacent left, L; adjacent right, R; opposite, O. Within the +/+ group, analysis of differences of least squares means revealed a significant difference between training quadrant and the other three quadrants ($t(36) > 2.9$, $p < 0.006$; indicated by asterisk). Within the −/− group, the differences between training quadrant and the other three quadrants were not statistically significant ($t(32) < 1.6$, $p > 0.11$). (C) The number of platform crossings during probe trial was examined. Within the +/+ group, analysis of differences of least squares means revealed a significant difference between training quadrant and quadrants L and O ($t(36) > 2.1$, $p < 0.04$, indicated by asterisk). The difference between T and R was not as pronounced ($t(36) = 1.98$, $p = .055$). Within the −/− group, the differences between training quadrant and the other three quadrants were not statistically significant ($t(32) < 0.73$, $p > 0.47$). No significant difference was observed between groups. (D) Shown is the escape latency during platform reversal test when platform was placed in training quadrant, T, or opposite quadrant, O. Analysis by paired t test revealed a significant difference between quadrant T and O for the +/+ mice ($t(9) = 5.4$; $p < 0.0001$, indicated by asterisk), but not for the −/− mice ($t(8) = 1.45$; $p = 0.19$.) The difference between groups was not statistically significant. (E) The performance of +/+ and −/− mice was the same during more intensive training, 3 blocks of 4 trials per day for 3 days. Repeated measures analysis of variance revealed no statistical difference between groups ($F(1,12) = 0.045$; $p = 0.83$; +/+, n = 7; −/−, n = 7). All error bars represent SEM.

bock et al., 1998), and release of neurotransmitter likely ejects protons into the synaptic cleft (DeVries, 2001; Krishtal et al., 1987; Traynelis and Chesler, 2001). In hippocampal slices, Krishtal et al. (1987) measured a brief (few ms) extracellular acidification accompanying EPSPs. Although the measured acid transients were relatively small (<0.2 pH units), localized changes in the microdomain of the synaptic cleft might be more pro-

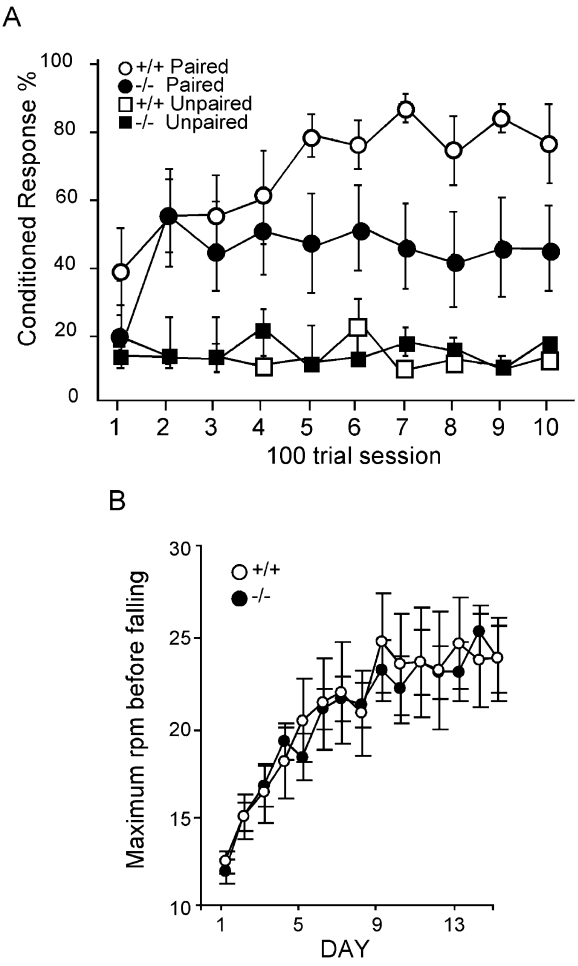

Figure 8. Eyeblink Conditioning Is Substantially Impaired and Rotarod Performance Is Normal in ASIC Knockout Mice

(A) The percentage of conditioned responses was determined for each 100 trial session. An analysis of variance revealed a significant interaction of the group (+/+ versus −/−) and condition (Paired versus Unpaired) factors, $F(1, 19) = 4.657$, $p < 0.05$. Post-hoc tests (Tukey HSD) revealed a significantly greater difference between paired and unpaired groups in the +/+ mice ($p < 0.05$), but not in the −/− mice. The results indicate that the +/+ mice developed greater associative eyeblink conditioning relative to the −/− mice. (B) The performance of +/+ and −/− mice is similar on the accelerating rotarod 0.3 rpm/s. Mice received three trials per day. Initial speed was 3 rpm. Averaged maximum rpm achieved before falling is plotted versus the day of the trials (+/+, n = 17; −/−, n = 19).

nounced. Moreover, a pair of sequential stimuli reduced pH further (Krishtal et al., 1987), suggesting that acidification might be more prominent when multiple vesicles are released within a short time, for example during HFS. Consistent with this proposal, DeVries recently found that exocytosed protons could suppress presynaptic Ca^{2+} currents in retinal cone receptors (DeVries, 2001). Our results identify ASIC as a key component of the hippocampal channels that open in response to extracellular acid. The data also place ASIC in the synapse. Thus, ASIC may be a postsynaptic target for protons released during synaptic transmission. Measurement of rapid pH changes in the synaptic cleft could provide a direct test for this model. Although this goal will be technically challenging, our studies heighten the need for such experiments.

In contrast to ASIC, protons inhibit the NMDA receptor (Tang et al., 1990; Traynelis and Cull-Candy, 1990). Therefore, the rapid acid transient noted by Kristal (Krishtal et al., 1987) might be expected to inhibit NMDA receptor function (Saybasili, 1998). In addition, the slower alkaline wave that presumably follows the initial acid transient may facilitate NMDA receptor activation (Gottfried and Chesler, 1994). Interestingly, the H^+-dependent inhibition of the NMDA receptor occurs at pH values (i.e., pH 6.5) that are known to activate ASIC (Traynelis and Cull-Candy, 1990). Thus we speculate that ASIC might serve to counterbalance the inhibitory effects of protons on synaptic transmission during the rapid acid transient.

Although protons are the only known activators of ASIC, it is possible that other ligands may activate or modulate currents from these channels. For example, the neurotransmitter FMRFamide (Phe-Met-Arg-Phe-NH_2) activates the closely related FaNaCh channel (Lingueglia et al., 1995), which plays a role in invertebrate synaptic transmission (Cottrell et al., 1992). Interestingly, FMRFamide and the mammalian neuropeptide FF (NPFF) also modulate the response of ASIC channels to acid, generating a sustained component of current that follows the initial transient current (Askwith et al., 2000). In rodents, central administration of FMRFamide, FMRFamide-related peptides, or antisera to these peptides alters behaviors such as learning and memory (Kavaliers and Colwell, 1993). We speculate that the effects of these peptides on learning could be mediated in part through ASIC activation. Recent data suggest that Zn^{2+} may also increase acid-evoked currents in channels composed of ASIC and BNC1α (Baron et al., 2001). The presence of high Zn^{2+} concentrations in presynaptic vesicles of hippocampal glutamatergic neurons (Slomianka, 1992) suggests that Zn^{2+} might enhance the synaptic function of these channels. Interestingly, like protons, Zn^{2+} also blocks the NMDA receptor (Westbrook and Mayer, 1987).

Contribution of H^+-Gated Currents to Learning and Memory

Our findings in the hippocampus led us to test the hypothesis that H^+-gated channels influence learning and memory. We found that ASIC null mice exhibited a mild deficit in spatial memory and a severe deficit in classical eyeblink conditioning. These two tasks depend on the hippocampus and cerebellum where ASIC is normally expressed (García-Añoveros et al., 1997; Waldmann et al., 1997b; and Figure 1) and where H^+-gated currents have been identified (Escoubas et al., 2000; Vyklicky et al., 1990; and Figure 4). The relationship between hippocampal LTP and behavioral tests of learning and memory remains uncertain (Martin et al., 2000). However, in −/− animals, the deficit in hippocampal LTP was accompanied by a hippocampus-dependent behavioral deficit.

The degree of impairment in cerebellum-dependent eyeblink conditioning was particularly pronounced in ASIC −/− animals and comparable to that observed in Purkinje cell degeneration (pcd) mutant mice (Chen et

al., 1996). Those mice exhibit a selective loss of Purkinje cells, the sole output from the cerebellar cortex, and they are functionally equivalent to animals with complete cerebellar cortical lesions. Interestingly, pcd mice are ataxic (Chen et al., 1996), as is often the case with impaired cerebellar function. In contrast, ASIC null mice ambulated normally and demonstrated normal motor learning on the accelerating rotarod. Therefore, the ASIC mutation may affect only specific types of learning.

The most plausible mechanism of learning-related plasticity in the cerebellar cortex is long-term depression (LTD) between granule and Purkinje cells (Mauk et al., 1998). These cells represent a key point of convergence between the neural pathways that carry the conditioned and unconditioned stimuli. Interestingly, mature Purkinje cells do not express functional NMDA receptors (Llano et al., 1991). However, LTD does require postsynaptic membrane depolarization and increased postsynaptic Ca^{2+} concentrations (Linden, 1994), features shared between cerebellar LTD and hippocampal LTP.

ASIC May Provide a Target for Pharmacological Modulation of Excitatory Neurotransmission

Agents that enhance synaptic activity, such as NMDA receptor agonists, have been explored as treatments to improve memory function (Muller et al., 1994). Involvement of ASIC in synaptic plasticity suggests that its activity might be manipulated for pharmacological purposes. In addition, ASIC might be inhibited to minimize the adverse consequences of acidosis. Both acidosis and high extracellular glutamate levels have been implicated in the pathology of seizures and stroke and the NMDA receptor may play a key role in the associated excitotoxicity (Choi, 1987; Obrenovitch et al., 1988). NMDA receptor antagonists have been explored as treatments for these conditions, but side effects have proven intolerable (During et al., 2000; Schehr, 1996). However, ASIC antagonists might provide a way to dampen excitatory transmission without inhibiting other key components of the system; thus ASIC antagonists might have less adverse effects than NMDA receptor antagonists. Supporting this speculation, ASIC disruption had no drastic consequences on animal development, viability, or baseline synaptic transmission. In contrast, targeted disruptions or hypomorphic alleles of the NMDA receptor are lethal or lead to severe behavioral abnormalities (Mohn et al., 1999). We speculate that ASIC may offer a novel pharmacological target for modulating excitatory neurotransmission.

Experimental Procedures

Generation of ASIC Knockout Mice

ASIC knockout mice were generated by homologous recombination in embryonic stem cells using a standard approach similar to that previously reported (Price et al., 2001). In the knockout allele, a PGK-neo cassette replaces the first exon of the *ASIC* gene and approximately 400 bp of upstream sequence.

Antibodies

The anti-ASIC$\alpha\beta$ antibody (Ab 6.4) was generated by injecting rabbits with a bacterially expressed thioredoxin fusion protein from pET32b (Novagen) containing the amino acids 459–528 of human ASIC (numbering as in García-Añoveros et al., 1997) (Pocono Rabbit Farm & Laboratory, Inc.). The anti-ASICα, (Ab MELK) and anti-ASICβ (Ab MELD) antibodies were generated by injecting sheep with the synthesized peptides MELKTEEEEVGGVQPVSIQAFA or MELDEGD SPRDLVAFANSCTLH, which correspond to the first 22 amino acids of mASICα and mASICβ, respectively (Elmira Biologicals). Affinity-purified antibodies were generated by absorbing sera to the specific immunogen coupled to Affi-Gel 10 or Affi-Gel 15 (Bio-Rad), washing with PBS, eluting with 50 mM glycine-HCl pH 2.5, neutralizing with Tris buffer pH 10.4, and stored in 1% BSA/PBS at 4°C or −20°C. Anti-PSD-95 monoclonal and anti-GluR2/3 antibodies were used according to the recommendations of the manufacturer (Sigma).

Immunoblotting and Immunoprecipitation

Synaptosomal fractionation and analysis were performed as described previously (Hruska-Hageman et al., 2001). For additional studies, Cos-7 cells transfected by electroporation (mASICα or mASICβ subcloned as Cla I-Kpn I fragments into pMT3), whole mouse brains, or dissected hippocampi were homogenized in phosphate-buffered saline (PBS) with 1% Triton X-100 plus protease inhibitors and centrifuged (10 min 700 × g) to remove particulate debris. The supernatant was Western blotted with the indicated antibodies or used for immunoprecipitation. For immunoprecipitation, 1 μl of undiluted affinity-purified Ab 6.4 was added to 750 μl of protein extract, incubated overnight with agitation at 4°C, precipitated with Protein A sepharose 50 μl (Pierce, 15 mg/ml) for 1 hr, resuspended in sample buffer (0.125 mM Tris, pH 7.5, 3.4% SDS, 17% glycerol, 67 mM dithiothreitol, 0.008% bromphenol blue), boiled 5 min, and Western blotted with the indicated antibodies. For Western blots or immunoprecipitation, equivalent amounts of protein extract were used.

Immunofluorescent Staining

Rat E18 hippocampal neurons (Gregory Brewer, Southern Illinois University School of Medicine, Springfield, IL) in primary culture for 4–8 days were transfected as described (Hruska-Hageman et al., 2001) with 1.6 μg hASIC (tagged with the FLAG epitope at the extreme N terminus and subcloned into pcDNA3.1 [Invitrogen]), in combination with an equal amount of pGreen Lantern-1 (Gibco BRL) or PSD-95-GFP (kind gift of D. Bredt) (Craven et al., 1999) or with N-terminal GFP-tagged ASIC in pEGFP (Clontech). At days 8–14, neurons were fixed at room temperature for 10–15 min in PBS plus 4% formaldehyde, 4% sucrose, permeabilized with 0.25% Triton X-100 in PBS for 5 min at room temperature, washed twice for 5 min in PBS, and incubated at room temperature for 2 hr with the M2 anti-FLAG antibody (International Biotechnologies, 1:600 in 3% BSA/PBS). Cells were washed in PBS, incubated for 1 hr at 37°C with Cy3-conjugated anti-mouse antibody (Jackson ImmunoResearch, Inc., 1:300), washed again, mounted with Vectashield (Vector Labs), and visualized by scanning confocal microscopy.

Whole-Cell Voltage-Clamp Experiments

Mouse hippocampal cultures were generated from postnatal day 1–2 pups (Mennerick et al., 1995) with the addition of insulin-transferrin-sodium selenite to the culture media (Sigma I-1884, resuspended in 50 ml H_2O, 2.5 μl was added per ml of media). Whole-cell patch-clamp was performed on large pyramidal neurons cultured for 1 to 2 weeks. Electrodes (4–7 MΩ) were filled with the intracellular solution containing (in mM): 120 KCl, 10 NaCl, 2 $MgCl_2$, 5 EGTA, 10 4-(2-hydroxyethyl)-1-piperazineethanesulfonic acid (HEPES), and 2 ATP. The pH was adjusted to 7.2 with tetramethylammonium hydroxide (TMA-OH) and osmolarity with tetramethylammonium chloride (TMA-Cl). Extracellular solutions contained (in mM): 128 NaCl, 1.8 $CaCl_2$, 5.4 KCl, 5.55 glucose, 10 HEPES, and 10 2-(4-morpholino)-ethanesulfonic acid (MES), and 1 μM tetrodotoxin. pH was adjusted to 7.4 or 5 with TMA-OH and osmolarity normalized with TMA-Cl. Neurons were held at −80 mV during recording. For experiments involving Mg^{2+} block of the NMDA receptor, pipette solutions contained (in mM): 140 $CsCl_2$, 4 NaCl, 10 HEPES, 0.5 $CaCl_2$, 5 EGTA, and extracellular solutions contained 140 NaCl, 2.8 KCl, 2 $CaCl_2$, and 10 HEPES. $MgCl_2$ (1 mM) and NMDA (200 μM) plus glycine (1 μM) were added as indicated.

Hippocampal Slice Recordings

Transverse hippocampal slices (350–400 μm) were prepared from 2- to 4-month-old mice. The slices were sectioned in ice-cold artificial cerebrospinal fluid (ACSF) containing (in mM): 119 NaCl, 2.5 KCl, 2.5 $CaCl_2$, 1.0 NaH_2PO_4, 1.3 $MgSO_4$, 26.2 $NaHCO_3$, 11 glucose, pH 7.4, bubbled with 95% O_2/5% CO_2, and incubated at 31°C for 2–5 hr before recording. Standard extracellular field potential recording techniques were performed in a submerged chamber, maintained at 31°C ± 0.5°C. Field postsynaptic excitatory potentials (EPSPs) were evoked with a bipolar stainless steel electrode at the border of CA3-CA1 subfields and recorded with 3 M NaCl-filled glass pipettes (<5 MΩ). A 100 μs test stimulation was delivered every 30 s by a stimulus isolation unit (Grass, SD9, MA). Input-output curves were obtained by plotting the stimulus voltage against the amplitude of EPSPs. All slices exhibited EPSPs of ≥1 mV in amplitude. The experimenter was blinded to genotype. Stimulus intensity was adjusted to evoke half-maximal responses. LTP was induced by a high-frequency stimulation (HFS, 100 Hz, 1 s, at test intensity). LTP was measured by normalizing the EPSP slopes after HFS to the mean slope of the baseline EPSP before HFS. Unless otherwise noted, two-sample t test was used to calculate statistical significance.

Morris Water Maze

The standard hidden platform version of the Morris water maze (Morris, 1981; Abeliovich et al., 1993) was used in two training protocols. In the first protocol, mice were given a single trial per day for 11 consecutive days. The second protocol consisted of three blocks of four trials per day for 3 consecutive days. The probe trials were similar to training trials except the platform was removed from the pool. The observer was blinded to genotype.

Eyeblink Conditioning

Conditioning was as described previously (Freeman and Nicholson, 2000) with the following modifications. The +/+ (n = 12) and −/− (n = 12) mice were given i.p. injections of Nembutal® (1.6 ml/kg) and atropine sulfate (0.67 mg/kg) for anesthesia. The mice were assigned to one of four experimental groups: +/+ paired (n = 6), −/− paired (n = 6), +/+ unpaired (n = 6), and −/− unpaired (n = 6). In the paired condition, the mice were given 100 presentations of a tone-conditioned stimulus (CS, 300 ms, 75 dB SPL, 2.0 kHz) and a shock unconditioned stimulus (US, 25 ms, 2.0 mA). The CS coterminated with the US, yielding an interstimulus interval of 275 ms. Paired training trials were separated by a variable intertrial interval that averaged 30 s (range = 18–42 s). In the unpaired condition, the mice were given explicitly unpaired presentations of the CS and US. The intertrial interval for unpaired training averaged 15 s (range = 9–21 s). Conditioned responses (CRs) were defined as responses that crossed a threshold of 0.4 units (amplified and integrated units) above baseline during the CS period after 80 ms.

Accelerating Rotarod

After accommodation to the apparatus (Columbus Instruments, Columbus, Ohio), three trials per day were performed for 15 days. A trial consisted of 10 s at constant speed (3 rpm), followed by constant acceleration at 0.3 rpm per s until falling.

Acknowledgments

We thank Melissa Redeker, Shannon Davison-Haigh, Mark Bainbridge, and Matt Thoendel for excellent assistance. We thank Roger Williamson and Ron Hrstka for help generating ASIC null mice. We thank David Bredt for PSD-95 GFP clone. We thank Charles Zorumski, Steve Mennerick, and Ann Benz for the mouse hippocampal neuron culture technique. We thank Steve Moore for reviewing the brain histology. We thank the University of Iowa DNA Core Facility (NIH # DK25295) and the Central Microscopy Research Facility for assistance. We acknowledge Dr. Jianguo Chen for his critical contributions in the development and design of the slice recording experiments, and for performing them in their entirety. This work was supported by the HHMI (M.J.W.), Veteran's Administration Research Career Development Award (J.A.W.), NINDS Grant NS38890 (J.H.F.), NIH grants GM57654, HL 64645, and HL14388 (T.H. and J.C.). C.C.A. and A.M.H.-H. are Associates and M.J.W. is an Investigator of the HHMI.

Received: July 26, 2001
Revised: March 7, 2002

References

Abeliovich, A., Paylor, R., Chen, C., Kim, J.J., Wehner, J.M., and Tonegawa, S. (1993). PKC gamma mutant mice exhibit mild deficits in spatial and contextual learning. Cell *75*, 1263–1271.

Askwith, C.C., Cheng, C., Ikuma, M., Benson, C.J., Price, M.P., and Welsh, M.J. (2000). Neuropeptide FF and FMRFamide potentiate acid-evoked currents from sensory neurons and proton-gated DEG/ENaC channels. Neuron *26*, 133–141.

Baron, A., Schaefer, L., Lingueglia, E., Champigny, G., and Lazdunski, M. (2001). Zn^{2+} and H^+, coactivators of acid sensing ion channels (ASIC). J. Biol. Chem. *276*, 35361–35367.

Bassilana, F., Champigny, G., Waldmann, R., de Weille, J.R., Heurteaux, C., and Lazdunski, M. (1997). The acid-sensitive ionic channel subunit ASIC and the mammalian degenerin MDEG form a heteromultimeric H^+-gated Na^+ channel with novel properties. J. Biol. Chem. *272*, 28819–28822.

Ben-Ari, Y., Aniksztejn, L., and Bregestovski, P. (1992). Protein kinase C modulation of NMDA currents: an important link for LTP induction. Trends Neurosci. *15*, 333–339.

Benson, C.J., Xie, J., Wemmie, J.A., Price, M.P., Henss, J.M., Welsh, M.J., and Snyder, P.M. (2002). Heteromultimerics of DEG/ENaC subunits form H^+-gated channels in mouse sensory neurons. Proc. Natl. Acad. Sci. USA *99*, 2338–2343.

Bliss, T.V., and Collingridge, G.L. (1993). A synaptic model of memory: long-term potentiation in the hippocampus. Nature *361*, 31–39.

Chen, L., and Huang, L.Y. (1992). Protein kinase C reduces Mg2+ block of NMDA-receptor channels as a mechanism of modulation. Nature *356*, 521–523.

Chen, L., Bao, S., Lockard, J.M., Kim, J.K., and Thompson, R.F. (1996). Impaired classical eyeblink conditioning in cerebellar-lesioned and Purkinje cell degeneration (pcd) mutant mice. J. Neurosci. *16*, 2829–2838.

Chen, C.C., England, S., Akopian, A.N., and Wood, J.N. (1998). A sensory neuron-specific, proton-gated ion channel. Proc. Natl. Acad. Sci. USA *95*, 10240–10245.

Chesler, M., and Kaila, K. (1992). Modulation of pH by neuronal activity. Trends Neurosci. *15*, 396–402.

Cho, K.O., Hunt, C.A., and Kennedy, M.B. (1992). The rat brain postsynaptic density fraction contains a homolog of the Drosophila discs-large tumor suppressor protein. Neuron *9*, 929–942.

Choi, D.W. (1987). Ionic dependence of glutamate neurotoxicity. J. Neurosci. *7*, 369–379.

Cottrell, G.A., Lin, J.W., Llinas, R., Price, D.A., Sugimori, M., and Stanley, E.F. (1992). FMRFamide-related peptides potentiate transmission at the squid giant synapse. Exp. Physiol. *77*, 881–889.

Craven, S.E., El-Husseini, A.E., and Bredt, D.S. (1999). Synaptic targeting of the postsynaptic density protein PSD-95 mediated by lipid and protein motifs. Neuron *22*, 497–509.

DeVries, S.H. (2001). Exocytosed protons feedback to suppress the Ca(2+) current in mammalian cone photoreceptors. Neuron *32*, 1107–1117.

De Zeeuw, C.I., Hansel, C., Bian, F., Koekkoek, S.K., van Alphen, A.M., Linden, D.J., and Oberdick, J. (1998). Expression of a protein kinase C inhibitor in Purkinje cells blocks cerebellar LTD and adaptation of the vestibulo-ocular reflex. Neuron *20*, 495–508.

During, M.J., Symes, C.W., Lawlor, P.A., Lin, J., Dunning, J., Fitzsimons, H.L., Poulsen, D., Leone, P., Xu, R., Dicker, B.L., et al. (2000). An oral vaccine against NMDAR1 with efficacy in experimental stroke and epilepsy. Science *287*, 1453–1460.

Escoubas, P., De Weille, J.R., Lecoq, A., Diochot, S., Waldmann, R., Champigny, G., Moinier, D., Menez, A., and Lazdunski, M. (2000).

Isolation of a tarantula toxin specific for a class of proton-gated Na+ channels. J. Biol. Chem. *275*, 25116–25121.

Freeman, J.H.J., and Nicholson, D.A. (2000). Developmental changes in eye-blink conditioning and neuronal activity in the cerebellar interpositus nucleus. J. Neurosci. *20*, 813–819.

García-Añoveros, J., Derfler, B., Neville-Golden, J., Hyman, B.T., and Corey, D.P. (1997). BNaC1 and BNaC2 constitute a new family of human neuronal sodium channels related to degenerins and epithelial sodium channels. Proc. Natl. Acad. Sci. USA *94*, 1459–1464.

Gottfried, J.A., and Chesler, M. (1994). Endogenous H+ modulation of NMDA receptor-mediated EPSCs revealed by carbonic anhydrase inhibition in rat hippocampus. J. Physiol. *478*, 373–378.

Gruol, D.L., Barker, J.L., Huang, L.Y., MacDonald, J.F., and Smith, T.G., Jr. (1980). Hydrogen ions have multiple effects on the excitability of cultured mammalian neurons. Brain Res. *183*, 247–252.

Hruska-Hageman, A.M., Wemmie, J.A., Price, M.P., and Welsh, M.J. (2002). Interaction of the synaptic protein PICK1 with the non-voltage gated sodium channels BNC1 and ASIC. Biochem. J. *361*, 433–445.

Huang, Y.Y., Wigstrom, H., and Gustafsson, B. (1987). Facilitated induction of hippocampal long-term potentiation in slices perfused with low concentrations of magnesium. Neurosci. *22*, 9–16.

Kavaliers, M., and Colwell, D.D. (1993). Neuropeptide FF (FLQPQRFamide) and IgG from neuropeptide FF antiserum affect spatial learning in mice. Neurosci. Lett. *157*, 75–78.

Kleschevnikov, A.M., and Routtenberg, A. (2001). PKC activation rescues LTP from NMDA receptor blockade. Hippocampus *11*, 168–175.

Krishtal, O.A., and Pidoplichko, V.I. (1981). A 'receptor' for protons in small neurons of trigeminal ganglia: possible role in nociception. Neurosci. Lett. *24*, 243–246.

Krishtal, O.A., Osipchuk, Y.V., Shelest, T.N., and Smirnoff, S.V. (1987). Rapid extracellular pH transients related to synaptic transmission in rat hippocampal slices. Brain Res. *436*, 352–356.

Linden, D.J. (1994). Long-term synaptic depression in the mammalian brain. Neuron *12*, 457–472.

Lingueglia, E., Champigny, G., Lazdunski, M., and Barbry, P. (1995). Cloning of the amiloride-sensitive FMRFamide peptide-gated sodium channel. Nature *378*, 730–733.

Lingueglia, E., de Weille, J.R., Bassilana, F., Heurteaux, C., Sakai, H., Waldmann, R., and Lazdunski, M. (1997). A modulatory subunit of acid sensing ion channels in brain and dorsal root ganglion cells. J. Biol. Chem. *272*, 29778–29783.

Llano, I., Marty, A., Armstrong, C.M., and Konnerth, A. (1991). Synaptic- and agonist-induced excitatory currents of Purkinje cells in rat cerebellar slices. J. Physiol. *434*, 183–213.

Malenka, R.C. (1991). Postsynaptic factors control the duration of synaptic enhancement in area CA1 of the hippocampus. Neuron *6*, 53–60.

Malenka, R.C., Madison, D.V., and Nicoll, R.A. (1986). Potentiation of synaptic transmission in the hippocampus by phorbol esters. Nature *321*, 175–177.

Malinow, R., Mainen, Z.F., and Hayashi, Y. (2000). LTP mechanisms: from silence to four-lane traffic. Curr. Opin. Neurobiol. *10*, 352–357.

Mandell, J.W., and Banker, G.A. (1996). A spatial gradient of tau protein phosphorylation in nascent axons. J. Neurosci. *16*, 5727–5740.

Martin, S.J., Grimwood, P.D., and Morris, R.G. (2000). Synaptic plasticity and memory: an evaluation of the hypothesis. Annu. Rev. Neurosci. *23*, 649–711.

Mauk, M.D., Garcia, K.S., Medina, J.F., and Steele, P.M. (1998). Does cerebellar LTD mediate motor learning? Toward a resolution without a smoking gun. Neuron *20*, 359–362.

Mennerick, S., Que, J., Benz, A., and Zorumski, C.F. (1995). Passive and synaptic properties of hippocampal neurons grown in microcultures and in mass cultures. J. Neurophysiol. *73*, 320–332.

Miesenbock, G., De Angelis, D.A., and Rothman, J.E. (1998). Visualizing secretion and synaptic transmission with pH-sensitive green fluorescent proteins. Nature *394*, 192–195.

Mohn, A.R., Gainetdinov, R.R., Caron, M.G., and Koller, B.H. (1999). Mice with reduced NMDA receptor expression display behaviors related to schizophrenia. Cell *98*, 427–436.

Morris, R.G. (1981). Spatial localization does not require the presence of local cues. Learn. Motiv. *12*, 239–260.

Muller, W.E., Scheuer, K., and Stoll, S. (1994). Glutamatergic treatment strategies for age-related memory disorders. Life Sci. *55*, 2147–2153.

Obrenovitch, T.P., Garofalo, O., Harris, R.J., Bordi, L., Ono, M., Momma, F., Bachelard, H.S., and Symon, L. (1988). Brain tissue concentrations of ATP, phosphocreatine, lactate, and tissue pH in relation to reduced cerebral blood flow following experimental acute middle cerebral artery occlusion. J. Cereb. Blood Flow Metab. *8*, 866–874.

Price, M.P., Snyder, P.M., and Welsh, M.J. (1996). Cloning and expression of a novel human brain Na^+ channel. J. Biol. Chem. *271*, 7879–7882.

Price, M.P., Lewin, G.B., McIlwrath, S.L., Cheng, C., Xie, J., Heppenstall, P.A., Stucky, C.L., Mannsfeldt, A.G., Brennan, T.J., Drummond, H.A., et al. (2000). The mammalian sodium channel BNC1 is required for normal touch sensation. Nature *407*, 1007–1011.

Price, M.P., McIlwrath, S.L., Xie, J., Cheng, C., Qiao, J., Tarr, D.E., Sluka, K.A., Brennan, T.J., Lewin, G.R., and Welsh, M.J. (2001). The DRASIC cation channel contributes to the detection of cutaneous touch and acid stimuli in mice. Neuron *32*, 1071–1083.

Saybasili, H. (1998). The protective role of mild acidic pH shifts on synaptic NMDA current in hippocampal slices. Brain Res. *786*, 128–132.

Schehr, R.S. (1996). New treatments for acute stroke. Nat. Biotechnol. *14*, 1549–1554.

Schulz, P.E., Cook, E.P., and Johnston, D. (1994). Changes in paired-pulse facilitation suggest presynaptic involvement in long-term potentiation. J. Neurosci. *14*, 5325–5337.

Shibuki, K., Gomi, H., Chen, L., Bao, S., Kim, J.J., Wakatsuki, H., Fujisaki, T., Fujimoto, K., Katoh, A., Ikeda, T., et al. (1996). Deficient cerebellar long-term depression, impaired eyeblink conditioning, and normal motor coordination in GFAP mutant mice. Neuron *16*, 587–599.

Slomianka, L. (1992). Neurons of origin of zinc-containing pathways and the distribution of zinc-containing boutons in the hippocampal region of the rat. Neurosci. *48*, 325–352.

Stowell, J.N., and Craig, A.M. (1999). Axon/dendrite targeting of metabotropic glutamate receptors by their cytoplasmic carboxy-terminal domains. Neuron *22*, 525–536.

Tang, C.M., Dichter, M., and Morad, M. (1990). Modulation of the N-methyl-D-aspartate channel by extracellular H+. Proc. Natl. Acad. Sci. USA *87*, 6445–6449.

Thompson, R.F., and Kim, J.J. (1996). Memory systems in the brain and localization of a memory. Proc. Natl. Acad. Sci. USA *93*, 13438–13444.

Traynelis, S.F., and Chesler, M. (2001). Proton release as a modulator of presynaptic function. Neuron *32*, 960–962.

Traynelis, S.F., and Cull-Candy, S.G. (1990). Proton inhibition of N-methyl-D-aspartate receptors in cerebellar neurons. Nature *345*, 347–350.

Tsien, J.Z., Huerta, P.T., and Tonegawa, S. (1996). The essential role of hippocampal CA1 NMDA receptor-dependent synaptic plasticity in spatial memory. Cell *87*, 1327–1338.

Varming, T. (1999). Proton-gated ion channels in cultured mouse cortical neurons. Neuropharmacol. *38*, 1875–1881.

Vyklicky, L.J., Vlachova, V., and Krusek, J. (1990). The effect of external pH changes on responses to excitatory amino acids in mouse hippocampal neurones. J. Physiol. (Lond.) *430*, 497–517.

Waldmann, R., and Lazdunski, M. (1998). H^+-gated cation channels: neuronal acid sensors in the NaC/DEG family of ion channels. Curr. Opin. Neurobiol. *8*, 418–424.

Waldmann, R., Champigny, G., Voilley, N., Lauritzen, I., and Lazdunski, M. (1996). The mammalian degenerin MDEG, an amiloride-sensitive cation channel activated by mutations causing neurodegeneration in *Caenorhabditis elegans*. J. Biol. Chem. *271*, 10433–10436.

Waldmann, R., Bassilana, F., de Weille, J.R., Champigny, G., Heurteaux, C., and Lazdunski, M. (1997a). Molecular cloning of a non-inactivating proton-gated Na^+ channel specific for sensory neurons. J. Biol. Chem. *272*, 20975–20978.

Waldmann, R., Champigny, G., Bassilana, F., Heurteaux, C., and Lazdunski, M. (1997b). A proton-gated cation channel involved in acid-sensing. Nature *386*, 173–177.

Westbrook, G.L., and Mayer, M.L. (1987). Micromolar concentrations of Zn^{2+} antagonize NMDA and GABA responses of hippocampal neurons. Nature *328*, 640–643.

Yu, X.M., and Salter, M.W. (1998). Gain control of NMDA-receptor currents by intracellular sodium. Nature *396*, 469–474.